Hindawi Publishing Corporation
Physics Research International
Volume 2014, Article ID 657271, 1 page
http://dx.doi.org/10.1155/2014/657271

Retraction

Retracted: Influence of Magnesium Substitution on Thermal and Electrical Properties of NiCuZn Ferrites for Microinductor Core Applications

Physics Research International

Received 2 October 2014; Accepted 2 October 2014; Published 30 October 2014

The paper titled "Influence of magnesium substitution on thermal and electrical properties of NiCuZn ferrites for microinductor core applications" [1], published in Physics Research International, has been retracted as it is found to contain a substantial amount of material from the paper "Studies on AC and DC electrical conductivity and thermoelectric power of NiMgCuZn ferrites" already published in International Journal of Nanoparticles, vol. 3, no. 4, pp. 349–366, 2010.

References

[1] M. Venkata Ramana, N. Ramamanohar Reddy, and K. V. Siva Kumar, "Influence of magnesium substitution on thermal and electrical properties of NiCuZn ferrites for microinductor core applications," *Physics Research International*, vol. 2012, Article ID 861690, 8 pages, 2012.

Hindawi Publishing Corporation
Physics Research International
Volume 2012, Article ID 861690, 8 pages
doi:10.1155/2012/861690

Research Article

Influence of Magnesium Substitution on Thermal and Electrical Properties of NiCuZn Ferrites for Microinductor Core Applications

M. Venkata Ramana,[1,2] N. Ramamanohar Reddy,[1] and K. V. Siva kumar[1]

[1] *Nanotechnology Laboratory, Department of Metallurgical and Materials Engineering, Indian Institute of Technology, Tamil Nadu, Chennai 600 036, India*
[2] *Ceramic Composite Materials Laboratory, Department of Physics, Sri Krishnadevaraya University, Ananthapur 505 003, India*

Correspondence should be addressed to M. Venkata Ramana, venkat6slr@gmail.com

Received 22 July 2011; Revised 7 January 2012; Accepted 12 January 2012

Academic Editor: Arcady Zhukov

Two series of NiMgCuZn ferrites, that is, (1) $Ni_xMg_{0.6-x}Cu_{0.1}Zn_{0.3}Fe_2O_4$ and sample G: $Ni_{0.3}Mg_{0.3-y}Cu_{0.1}Zn_{0.5-y}Fe_2O_4$ with $x = 0.0, 0.1, 0.2, 0.3$ and (2) $Ni_xMg_{0.6-x}Cu_{0.1}Zn_{0.3}Fe_2O_4$ with $y = 0.0, 0.1, 0.2$ were synthesized and prepared by conventional ceramic double-sintering process and to use them as core materials for microinductor applications. The formation of single phase was confirmed by X-ray diffraction. The temperature and compositional variation of DC, AC electrical conductivities (σ) and thermoelectric power (α) were studied on these two series of polycrystalline ferrospinels. The studies were carried out in wide range of temperature from 30 to 350°C. On the basis of thermoelectric study, the ferrites under present work were found to be shown as n-type and p-type transition. The electrical conduction in these ferrospinels is explained in the light of polaron hopping mechanism. These ferrite compositions have been developed for their use as core materials for microinductor applications.

1. Introduction

The polycrystalline NiMgCuZn soft ferrites are suitable for core materials in microinductor applications. In view of the extensive applications of NiCuZn ferrite [1–4], it is economical to replace nickel with magnesium and achieve desirable properties in NiMgCuZn ferrites. MgCuZn ferrite is a pertinent magnetic material suitable for high-frequency applications owing to its properties like high resistivity, fairly high Curie transition temperature, environmental stability, and low cost [5–8]. In the present investigation two series of NiMgCuZn ferrospinels were prepared, their temperature and compositional dependence of electrical properties like DC, AC electrical conductivities and Seebeck coefficient were studied, and the results were reported along with the conduction mechanism.

2. Experimental Procedure

2.1. Materials and Methods. Two series of soft ferrite compositions having the chemical formulas: (i) $Ni_xMg_{0.6-x}Cu_{0.1}Zn_{0.3}Fe_2O_4$, where $x = 0.0, 0.1, 0.2, 0.3$ and (ii) $Ni_{0.3}Mg_{0.3-y}Cu_{0.1}Zn_{0.5-y}Fe_2O_4$, where $y = 0.0, 0.1, 0.2$ were prepared employing analytical grade NiO, MgO, CuO, ZnO, and Fe_2O_3. These constituents were ball milled (Retsch PM-200, Germany) in acetone medium for 10 h and dried in an oven. These dried powders were calcined in the form of cakes in closed alumina crucibles at 800°C for 4 h. After presintering, these cakes were crushed and ball milled once again to obtain fine particles, and finally these powders were sieved to get uniform particle size. The presintered green powders were mixed with 2% PVA as a binder and were compacted in the form of pellets of 1.2 cm diameter and 2 mm thickness at 150 MPa. These compacted bodies were finally sintered at 1250°C for 2 h using a programmable furnace and were cooled to room temperature at the rate of 80°C/hr. Sufficient care was taken to avoid zinc loss during the sintering process. All the samples were structurally characterized using Philips high-resolution X-ray diffraction system PM1710 with Cu K_α radiation.

2.2. Experimental Details. DC electrical conductivity measurements were carried out by a cell having guard ring facility in addition to the two probes [9]. Silver paste (Du Pont) was applied to both the surfaces of the pellet to obtain good ohmic contacts. The measurements of conductivity were made by applying a constant voltage of 2 V from a regulated power supply, in the temperature range 30 to 350°C. The electrical conductivity (σ_{DC}) of NiMgCuZn ferrites under investigation has been computed using the relation

$$\sigma = \left(\frac{It}{VA}\right), \tag{1}$$

where I is the current passing through the specimen, V is the voltage applied to the specimen, t is the thickness of the sample, and A denotes the area of cross-section of the sample. The Curie transition temperature T_c of the samples was determined by magnetic permeability measurements [10]. Thermoelectric power (Seebeck coefficient) measurements were carried out in the temperature region 30 to 350°C by differential method similar to that of Reddy et al. [11] with a few modifications. A temperature difference of ΔT = 10 K was maintained across the sample with the help of a microfurnace fitted to the sample holder assembly. Temperatures of both the surfaces of the pellet were measured with precalibrated chromel-alumel thermocouples. The Thermoelectric power "α" was measured from the relation

$$\alpha = \frac{\Delta V}{\Delta T}. \tag{2}$$

Following convention adopted by Lal et al. [12] the positive sign indicates negative charge carriers and vice versa.

The AC conductivity, σ_{AC} of these ferrites were evaluated from the dielectric measurements (ε' and loss tangent, $\tan\delta$), carried out at 1 kHz employing a computer-controlled low-frequency impedance analyzer (Hioki 3532-50 LCR Hi Tester, Japan) using the standard formulae in the temperature range 30 to 350°C. In order to understand the electrical conduction mechanism, the dielectric measurements were carried out in the frequency region 100 Hz to 1 MHz and σ_{AC} that was evaluated.

3. Results and Discussion

Table 1 gives the details of various oxides present in the two series of NiMgCuZn ferrites in mole percent. Typical XRD patterns of one sample each from the two series of NiMgCuZn ferrites (samples—B and G) are presented in Figure 1. X-ray analysis of these ferrite samples reveals the single-phase spinel structure. The lattice parameters of these ferrites were calculated from d-spacings. The variation of lattice parameter with the composition in these two series of samples is given in Table 2. It can be observed from Table 2 that, in a given series, the lattice parameter is found to increase. The ionic radii of ions are Ni^{2+} = 0.72 Å, Mg^{2+} = 0.65 Å, Cu^{2+} = 0.72 Å, Zn^{2+}= 0.74 Å, and Fe^{2+} = 0.64 Å, respectively. The increasing trend of lattice constant in the two series of ferrites is attributed to the presence of Mg ion having a low ionic radius. The densities of the samples are presented in Table 2. In series 1 and 2 it can be noticed that when the nickel or magnesium concentrations are increased in the ferrites, the magnitude of density also increases.

Table 1: Composition of various components of NiMgCuZn ferrites in mole percent.

S. No.	Sample	NiO	MgO	CuO	ZnO	Fe_2O_3
Series 1						
(1)	A	0	30	5	15	50
(2)	B	5	25	5	15	50
(3)	C	10	20	5	15	50
(4)	D	15	15	5	15	50
Series 2						
(5)	E	15	5	5	25	50
(6)	F	15	10	5	20	50
(7)	G	15	15	5	15	50

Series 1: A: $Mg_{0.6}Cu_{0.1}Zn_{0.3}Fe_2O_4$, B: $Ni_{0.1}Mg_{0.5}Cu_{0.1}Zn_{0.3}Fe_2O_4$, C: $Ni_{0.2}Mg_{0.4}Cu_{0.1}Zn_{0.3}Fe_2O_4$, D: $Ni_{0.3}Mg_{0.3}Cu_{0.1}Zn_{0.3}Fe_2O_4$.
Series 2: E: $Ni_{0.3}Mg_{0.1}Cu_{0.1}Zn_{0.5}Fe_2O_4$, F: $Ni_{0.3}Mg_{0.2}Cu_{0.1}Zn_{0.4}Fe_2O_4$, and G: $Ni_{0.3}Mg_{0.3}Cu_{0.1}Zn_{0.3}Fe_2O_4$.

The room temperature values of DC, AC conductivities and Seebeck coefficients for the two series of the ferrospinels studied in the present work are also presented in Table 2 for comparison.

The variation of DC conductivity ($\log\sigma_{DC}$) with temperature is shown in Figures 2(a) and 2(b), and the variation of σ_{DC} with composition at room temperature is shown in Figure 2(c), for the series 1 and 2, respectively. The variation of DC conductivity with increase of temperature is almost linear in all the ferrites and shows a change of slope near 100 to 130°C. However, in all the ferrites studied in the present work, no slope change is noticed at Curie transition temperature. The activation energies are calculated from the following formula:

$$\sigma = \sigma_0 \exp\left(-\frac{E_{DC}}{kT}\right), \tag{3}$$

where E_{DC} is the activation energy, k is the Boltzmann constant, and T is the absolute temperature.

The activation energies in two regions calculated from the least square analysis of the data are given in Table 3.

An examination of data presented in Table 3 shows that, in sample A (sample without nickel) of series 1, the magnitudes of DC conductivity are high, and activation energy is found to be low compared to other ferrite samples. However, the addition of nickel decreases the conductivity and increases the activation energy in sample B. Further raise in nickel concentration in series 1 saturated the magnitudes of conductivity and decreased activation energies. In series 2

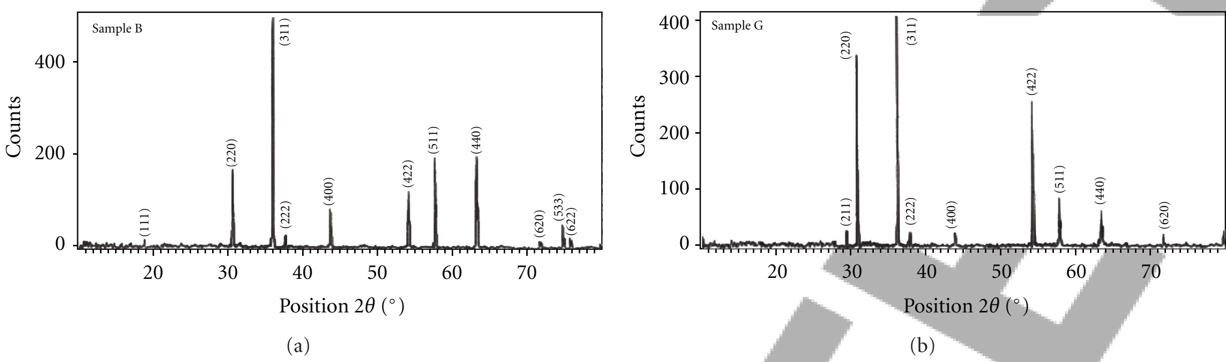

Figure 1: X-ray diffractograms of sample B: $Ni_xMg_{0.6-x}Cu_{0.1}Zn_{0.3}Fe_2O_4$ and sample G: $Ni_{0.3}Mg_{0.3-y}Cu_{0.1}Zn_{0.3-y}Fe_2O_4$.

Table 2: Values of AC, DC conductivities and Seebeck coefficient at room temperature.

S. No.	Sample	Lattice parameter Å	Density $kg \cdot m^{-3}$	σ_{DC} at RT $\Omega^{-1}Cm^{-1}$	σ_{AC} at RT $\Omega^{-1}Cm^{-1}$	Seebeck coefficient $\alpha\,\mu V/K$
(1)	A	8.374	4.267	7.467×10^{-5}	1.799×10^{-4}	−79.55
(2)	B	8.274	4.442	5.676×10^{-7}	2.247×10^{-6}	2168
(3)	C	8.255	4.665	4.425×10^{-6}	8.475×10^{-6}	1966
(4)	D	8.234	5.321	2.755×10^{-6}	2.292×10^{-6}	1586
(5)	E	8.260	4.498	3.790×10^{-6}	3.958×10^{-6}	4830
(6)	F	8.252	4.534	2.729×10^{-6}	2.446×10^{-6}	1741
(7)	G	8.234	5.321	2.755×10^{-6}	2.292×10^{-6}	1586

Table 3: It shows the activation energies of DC conductivity at room temperature.

S. No.	Sample	T_c (°C)	Activation energies of σ_{DC} (ev)		
			IR	ER	ΔE
(1)	A	230	0.599	0.141	0.458
(2)	B	270	1.025	0.726	0.298
(3)	C	290	1.026	0.467	0.559
(4)	D	300	1.113	0.386	0.727
(5)	E	210	0.855	0.536	0.319
(6)	F	280	1.008	0.428	0.580
(7)	G	300	1.113	0.386	0.727

IR: Intrinsic region, ER: Extrinsic Region, and T_c: Curie temperature.

with increase of magnesium and decrease of zinc contents, the activation energies increased in the intrinsic region while there is a decreasing trend of activation energy in extrinsic region. In series 1 as the nickel concentration is increased, the resistivity first increases and there after it decreases. This may be attributed to the fact that at low concentrations nickel exists in Ni^{2+} state, and it prefers A-site occupation. If the concentration of nickel is increased, Ni^{2+} converts into Ni^{3+} and goes to B sites due to their ionic sizes. However, since the copper concentration is maintained low, its contribution may be negligible. In series 2 the zinc concentration is more compared to series 1. Moreover, zinc ion has strong A-site preference. Due to the preferential occupation of zinc ions in A site it forces the nickel ions to occupy B sites. In view of this the conductivity increases in series 2. It can also be noticed from Table 3 that, in general, the activation energies of intrinsic region are larger than the activation energies of the extrinsic region. Generally the electric conductivity is controlled by the migration of charge species under the influence of electric field and by the defect ion complexes, the polarization field, the relaxations, and so forth. At lower temperatures the defect ion complexes, grain boundaries also contribute to the conduction mechanism. The activation energy is less in this region (i.e., extrinsic region). At high-temperatures the charge species may not be subjected to any internal field. The defect ion complexes tend to dissociate. The activation energy in the high-temperature region may be the migration energy for the charges.

AC conductivity σ_{AC} was evaluated from the data of dielectric constant (ε') and loss, $\tan\delta$ using the relation

$$\sigma_{AC} = \varepsilon' \varepsilon_o \omega \tan\delta, \quad (4)$$

where ε_o is the vacuum permittivity and ω the angular frequency.

The plots of AC conductivity ($\log \sigma_{AC}$) with reciprocal temperature are shown in Figures 3(a) and 3(b), and the variation of σ_{AC} with composition at room temperature is shown in Figure 3(c). It can be noticed from the figures that there are peak-like regions which indicate the Curie transition temperatures of the corresponding ferrite samples. Electrical conductivity studies on transition metal oxides [13], rare earth oxides [14–16], indicted polaron conduction mechanism through hopping.

In the first series of ferrites, namely, (samples A, B, C, and D) the nickel concentration is increased while the magnesium concentration is decreased keeping copper and zinc fixed. The variation of AC conductivity ($\log \sigma_{AC}$)

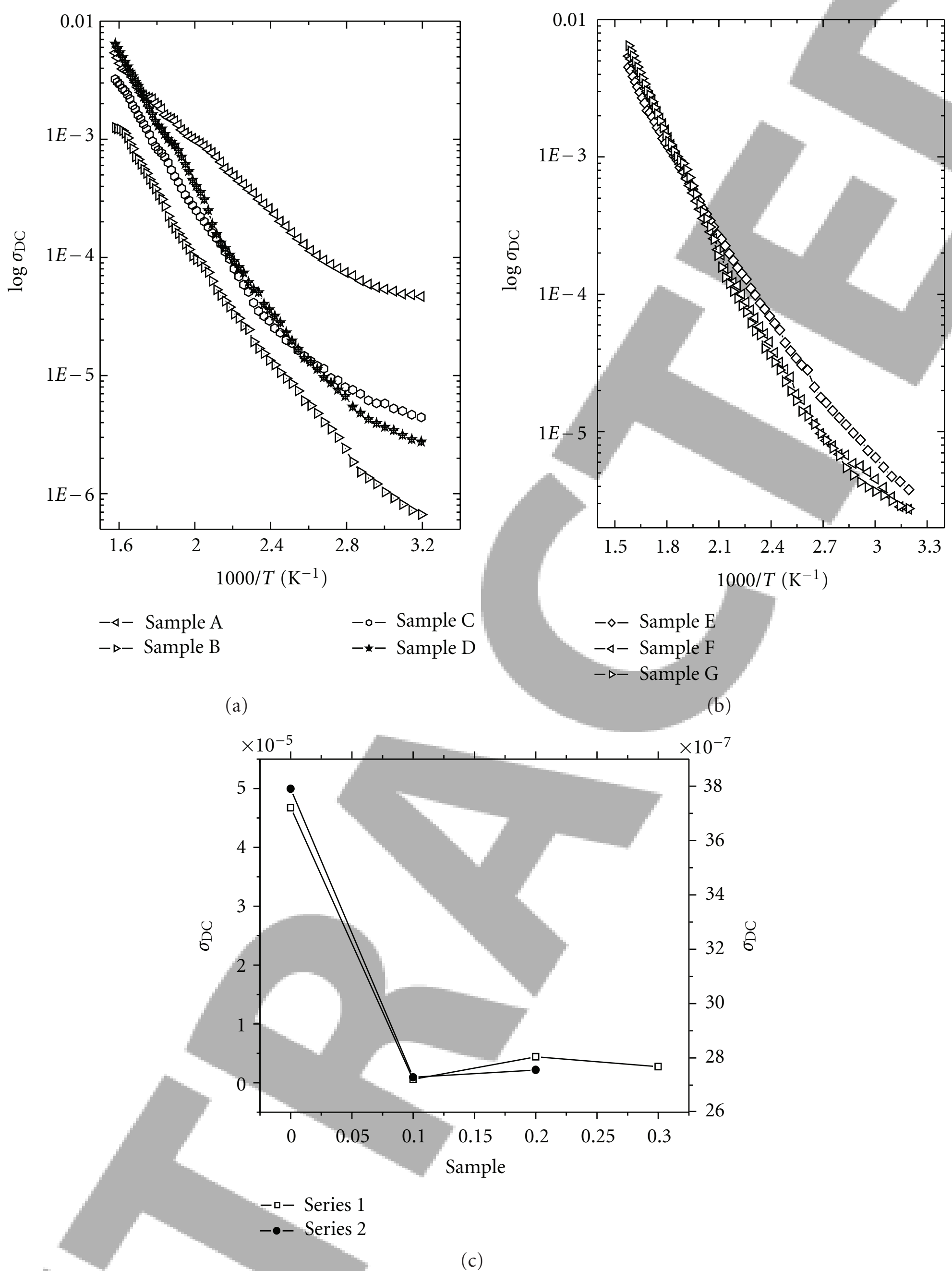

Figure 2: (a) Variation of $\log \sigma_{DC}$ with the T^{-1} for series 1. (b) Variation of $\log \sigma_{DC}$ with the T^{-1} for series 2. (c) Variation of $\log \sigma_{DC}$ with composition at room temperature.

with inverse temperature in these ferrites at the room temperature can be noticed from the figures that as the nickel concentration in the ferrite increases, the conductivity is low and found to be more with the addition of nickel in sample B further decreasing with increase of nickel content in series 1. However, the conductivity of series 2 is decreasing when magnesium and zinc concentration in the ferrite is varied keeping nickel and copper constant. The activation energy in the series 1 is found to be increasing in both paramagnetic and ferromagnetic region. While in series 2 it is decreasing in both the regions, it may also be noted that activation energies vary from 0.1 to 1.1, and a high activation energy goes hand in hand with a low conductivity of the ferrites as shown by Samokhralov and Rustmov [17].

Conduction by polarons is discussed by several workers [18–20]. Polarons are of two types: large and small polarons. In the large polaron model, the conductivity is by band mechanism at all temperatures, and the AC conductivity decreases with frequency. The small polarons conduct in band-like manner up to a certain temperature, and the

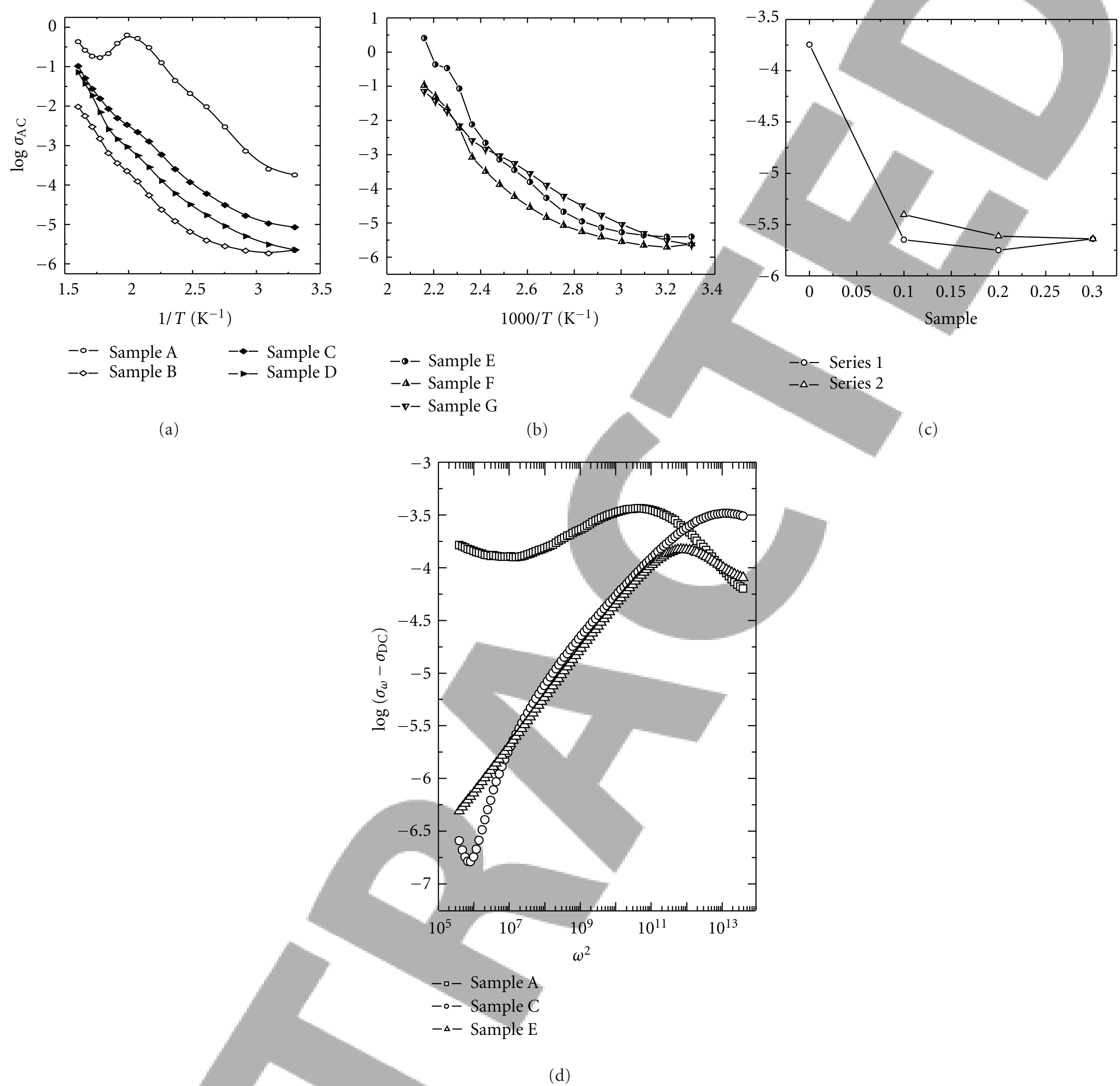

FIGURE 3: (a) Variation of $\log \sigma_{(AC)}$ with T^{-1} for series 1. (b) Variation of $\log \sigma_{(AC)}$ with T^{-1} for series 2. (c) Variation of $\log \sigma_{(AC)}$ with composition at room temperature. (d) Plots of $\log \sigma_{(AC\text{-}DC)}$ with $\log \omega^2$ one sample from each series.

conductivity shows an increase with frequency. At higher temperatures, the conduction is by thermally activated hopping mechanism. For small polaron model the conduction increases with the frequency, and follows the relation

$$\sigma_\omega - \sigma_{DC} = \frac{\omega^2 \tau^2}{(1 + \omega^2 \tau^2)}, \tag{5}$$

where ω is the angular frequency, and τ is the staying time ($\sim 10^{-10}$) for the frequencies $\omega^2 \tau^2 < 1$. $\log(\sigma_\omega - \sigma_{DC})$ versus $\log \omega^2$ that should be a straight line. Plot of $\log(\sigma_\omega - \sigma_{DC})$ as a function of $\log \omega^2$ at room temperature for three typical sample is shown in Figure 3(d). It can be seen that in the plot there are regions of decreasing, increasing of $\log(\sigma_\omega - \sigma_{DC})$ with increasing frequency. It is not conformation to equation (5). It can be stated that in the present series of ferrospinel samples the results tend to indicate that the conduction mechanism is due to mixed polaron hopping.

The variation of thermoelectric power with the temperature in the low- and high-temperature regions for two series of ferrites are shown in Figures 4(a) and 4(b), and variation at room temperature value can be observed in Figure 4(c). The thermoelectric voltage ΔV developed across the pellet

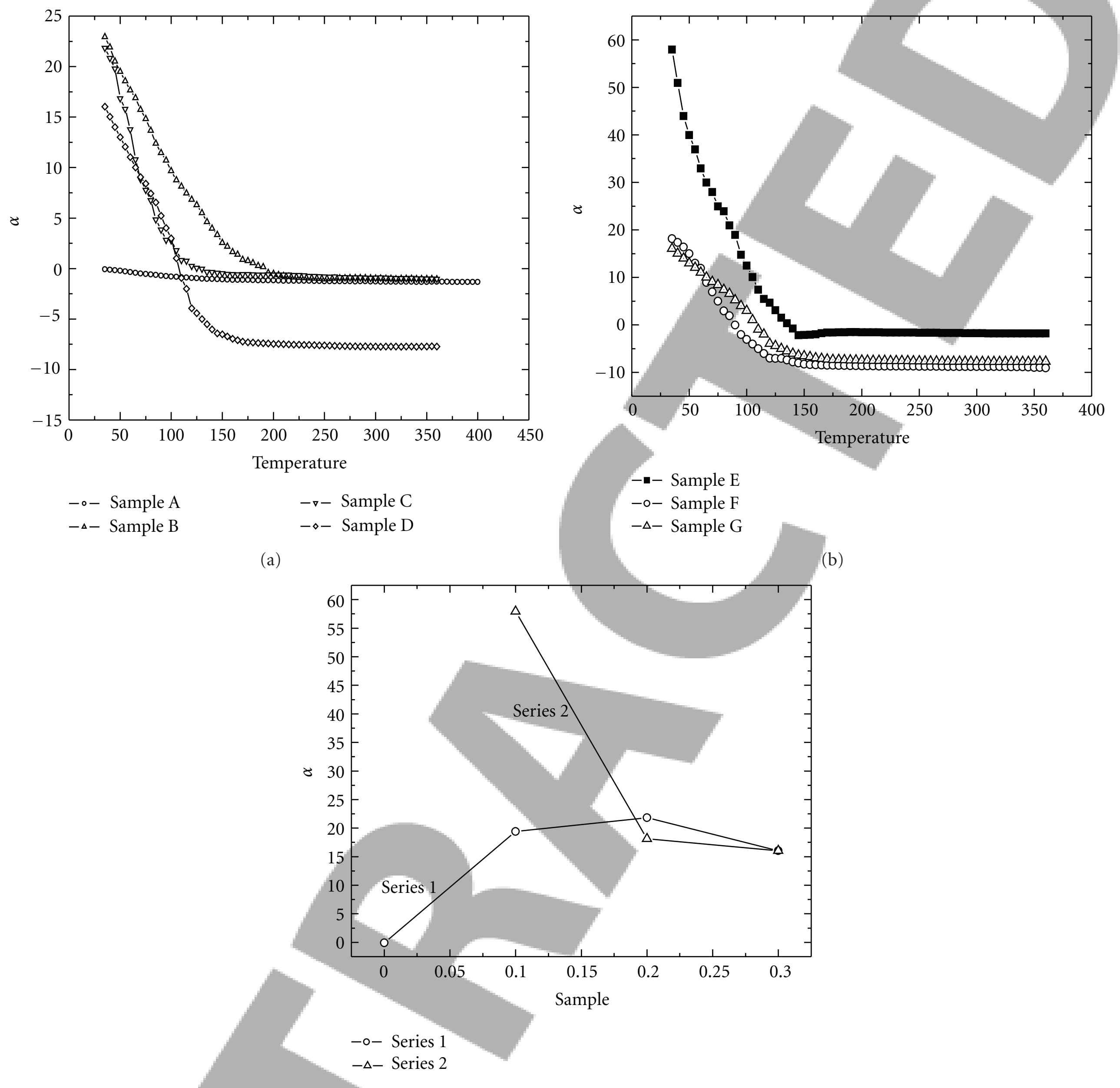

Figure 4: (a) Variation of the Seebeck coefficient with temperature for series 1. (b) Variation of the Seebeck coefficient with temperature for series 2. (c) Variation of Seebeck coefficient at room temperature for the two series of ferrites.

has a temperature gradient, and ΔT is shown as $\alpha = \Delta V/\Delta T$. The positive sign of α indicates negative charge carriers and vice versa.

It can be seen from Table 2, at room temperature the Seebeck coefficient of pure magnesium copper zinc ferrite (i.e., Sample A) shows negative sign, and with the addition of nickel the Seebeck coefficient α has increased showing that positive sign further increase of nickel composition leads to the reduction of α value. While in the series 2, the sign of the Seebeck coefficient at room temperature is negative only for the samples and decreases with increase of magnesium. However, it can be seen that the copper concentration is kept in concentration in both series. With the addition of nickel concentration, the thermoelectric power shows positive sign showing that from majority carriers n-type semiconductors it can be observed that as the temperature increases the Seebeck coefficient sign that shows positive sign, as such it behaves n-type and p-type semiconductors both the series 1 and 2 the same is observed. The temperature dependence of Seebeck coefficient (α) for the ferrites is satisfactorily described by the formula [21]

$$\alpha = A + \left(\frac{B}{T}\right), \quad (6)$$

where A and B are constants, and T is the temperature in K.

It can be seen from Table 2 that the sign of the Seebeck coefficient is transition from n-type and p-type semiconductors for all the ferrites on the basis of sign that the Ni substituted MgCuZn ferrites have been classified as n-type and p-type semiconductors. Thus, the conduction mechanism in these ferrites is predominantly due to hopping of electrons [22] from Fe^{2+} to Fe^{3+} ions

$$Fe^{3+} + e \Longleftrightarrow Fe^{2+}. \tag{7}$$

Ravinder [23] carried out the work and reported that the Seebeck coefficient is decreasing when nickel is increased, and this in turn leads to decrease in Zinc composition. All the mixed Ni-Zn ferrites are positive, and it shows that the majority of the charge carriers are holes. The presence of nickel on the octahedral sites favours the conduction mechanism [24]

$$Ni^{2+} + Fe^{3+} \Longleftrightarrow Ni^{3+} + Fe^{2+}. \tag{8}$$

The conduction mechanism in p-type samples is predominantly due to hole transfer from

$$Ni^{2+} \text{ to } Ni^{2+} \text{ ions}: \; Ni^{2+} + \; h \Longleftrightarrow Ni^{3+}. \tag{9}$$

It can be observed that Seebeck coefficient α is found to be decreasing in all the ferrites. Except in sample A it is increasing up to sample B and then starts decreasing due to the addition of nickel. All our results show good agreement with data from the literature.

4. Conclusions

The polycrystalline NiMgCuZn ferrite samples were prepared by the conventional method. X-ray diffraction patterns reveal the single phase spinel structure. The DC, AC and thermoelectric (Seebeck) coefficient was measured for these ferrospinels. The temperature variation of DC conductivity of series 1 indicates that the σ_{DC} is high and activation energy is low. In series 2, the activation energy is decreasing in extrinsic regions and increasing at the intrinsic region with increasing and decreasing of magnesium and zinc content in the present studied ferrites. The AC conductivity of these ferrites was calculated from the dielectric measurements. It indicates that the conduction mechanism is due to mixed polaron hopping. The temperature dependence of Seebeck coefficient of this ferrites is showing p-type and n-type semiconductor behavior.

Acknowledgments

This research was financially supported by Defence Research and Development Organization, (DRDO) under Grants ERIP/ER/0103301/M/1 dated 09.01.2002, New Delhi, India. The authors are thankful to Prof. A. Varadarajulu, Department of Polymer Science and Technology, Sri Krishnadevaraya University, Anantapur, A.P, India for valuable discussions in the preparation of the manuscript.

References

[1] C. G. Koops, "On the dispersion of resistivity and dielectric constant of some semiconductors at audiofrequencies," *Physical Review*, vol. 83, no. 1, pp. 121–124, 1951.

[2] G. Moltgen, "Dielectric analysis of ferrites," *Zeitschrift fur Angewandte Physik*, vol. 4, pp. 216–224, 1952.

[3] K. Iwauchi, "Dielectric properties of fine particles of Fe_3O_4 and some ferrites," *Japanese Journal of Applied Physics*, vol. 10, pp. 1520–1528, 1971.

[4] L. G. Van Uiteret, "Dielectric properties of and conductivity in ferrites ," *Proceedings of the IRE* , vol. 44, no. 10, pp. 1294–1303, 1956.

[5] N. Rezlescu, E. Rezlescu, P. D. Popa, M. L. Craus, and L. Rezlescu, "Copper ions influence on the physical properties of a magnesium-zinc ferrite," *Journal of Magnetism and Magnetic Materials*, vol. 182, no. 1-2, pp. 199–206, 1998.

[6] N. Rezlescu, L. Sachelarie, L. Rezlescu, and P. D. Popa, "Influence of PbO and Ta_2O_5 on some physical properties of MgCuZn ferrites," *Crystal Research and Technology*, vol. 36, no. 2, pp. 157–167, 2001.

[7] L. Sachelarie, E. Rezlescu, and N. Rezlescu, "Influence of PbO on some properties of MgCuZn ferrites," *Physica Status Solidi*, vol. 179, no. 1, pp. R1–R3, 2000.

[8] D. N. Bhosale, N. D. Choudhari, S. R. Sawant, and P. P. Bakare, "Initial permeability studies on high density Cu-Mg-Zn ferrites," *Journal of Magnetism and Magnetic Materials*, vol. 173, no. 1-2, pp. 51–58, 1997.

[9] V. R. K. Murthy and J. Sobhanadri, "Electrical conductivity of some nickel-zinc ferrites," *Physica Status Solidi*, vol. 38, no. 2, pp. 647–651, 1976.

[10] N. Varalaxmi, M. VenkataRamana, N. Ramamanohar Reddy, G. Rajitha, K. V. Sivakumar, and V. R. K. Murthy, in *Elastic behavior and internal friction of ferrospinels*, 2006.

[11] V. D. Reddy, M. A. Malik, and P. V. Reddy, "Electrical transport properties of manganese-magnesium mixed ferrites," *Materials Science and Engineering B*, vol. 8, no. 4, pp. 295–301, 1991.

[12] H. B. Lal, B. K. Verma, and V. Ram Yadav, "Electrical transport in heavy rare-earth iron garnets," *Journal of Materials Science*, vol. 17, no. 11, pp. 3317–3326, 1982.

[13] D. Adler and J. Feinleib, "Electrical and optical properties of narrow-band materials," *Physical Review B*, vol. 2, no. 8, pp. 3112–3134, 1970.

[14] G. V. S. Rao, S. Ramdas, P. N. Mehrotra, and C. N. R. Rao, "Electrical transport in rare-earth oxides," *Journal of Solid State Chemistry*, vol. 2, no. 3, pp. 377–384, 1970.

[15] H. B. Lal, B. K. Verma, and N. Dar, "On the Electrical Transport and Dielectric Properties of Heavy Rare–Earth Sesquioxides," *Indian Journal of Cryogenics*, vol. 1, pp. 119–126, 1976.

[16] H. B. Lal and N. Dar, "Magnetic susceptibility, electrical conductivity and dielectric constant of Er_2O_3," *Indian Journal of Pure and Applied Physics*, vol. 14, pp. 788–795, 1976.

[17] A. A. Samokhralov and A. G. Rustmov, *Soviet Physics, Solid State*, vol. 7, p. 961, 1965.

[18] J. Appel, in *Solid State Physics*, F. Seitz, D. Turnbull, and H. Ehrenreich, Eds., vol. 21, pp. 193–391, Academic press, New York, USA, 1968.

[19] I G. Austin and N. F. Mott, "Polarons in crystalline and non-crystalline materials," *Advances in Physics*, vol. 18, no. 71, pp. 41–102, 1969.

[20] N. F. Mott and E. A. Davis, *Phonons and Polarons in Electronics Processing in Non Crystalline Materials*, Clarendon Press, Oxford, UK, 1971.

[21] S. S. Flaschen and L. G. Van Uitert, "New low contact resistance electrode," *Journal of Applied Physics*, vol. 27, no. 2, p. 190, 1956.
[22] L. G. Van Uitert, "Dc resistivity in the nickel and nickel zinc ferrite system," *The Journal of Chemical Physics*, vol. 23, no. 10, pp. 1883–1887, 1955.
[23] D. Ravinder, "Electrical properties of zinc substituted nickel ferrites," *Indian Journal of Physics*, vol. 74, no. 3, pp. 331–333, 2000.
[24] J. Smit and H. P. J. Wijn, *Ferrites*, Cleaver, London, UK, 1959.